Article

Different Effects of Salt Bridges near the Active Site of Cold-Adapted *Proteus mirabilis* Lipase on Thermal and Organic Solvent Stabilities

VinayKumar Dachuri [1,2] **, Sei-Heon Jang** [1] **and ChangWoo Lee** [1,*]

[1] Department of Biomedical Science, Center for Bio-Nanomaterials, Daegu University, Gyeongsan 38453, Korea; dachurivinay@gmail.com (V.D.); shjang@daegu.ac.kr (S.-H.J.)
[2] Research Center for Herbal Convergence on Liver Disease, Daegu Haany University, Gyeongsan 38578, Korea
* Correspondence: leec@daegu.ac.kr; Tel.: +82-53-850-6464

Abstract: Organic solvent-tolerant (OST) enzymes have been discovered in psychrophiles. Cold-adapted OST enzymes exhibit increased conformational flexibility in polar organic solvents resulting from their intrinsically flexible structures. *Proteus mirabilis* lipase (PML), a cold-adapted OST lipase, was used to assess the contribution of salt bridges near the active site involving two arginine residues (R237 and R241) on the helix η1 and an aspartate residue (D248) on the connecting loop to the thermal and organic solvent stabilities of PML. Alanine substitutions for the ion pairs (R237A, R241A, D248A, and R237A/D248A) increased the conformational flexibility of PML mutants compared to that of the wild-type PML in an aqueous buffer. The PML mutants became more susceptible to denaturation after increasing the dimethyl sulfoxide or methanol concentration than after a temperature increase. Methanol was more detrimental to the structural stability of PML compared to dimethyl sulfoxide. These results suggest that direct interactions of dimethyl sulfoxide and methanol with the residues near the active site can have a destructive effect on the structure of PML compared with the global effect of heat on the protein structure. This study provides insight into the conformational changes within an OST enzyme with different effects on its thermal and organic solvent stabilities.

Keywords: catalysis; cold-adapted enzyme; conformational flexibility; organic solvent-tolerant enzyme; lipase; *Proteus mirabilis*; salt bridge; stability

1. Introduction

Organic solvents increase the solubility of non-water-soluble substrates in enzymatic reactions [1]. On the other hand, organic solvents also strip off water molecules from the surface of enzymes and penetrate deeper into the active site, causing denaturation of the protein structure [2,3]. The varying hydrophobicity of organic solvents has different effects on the activity of enzymes [4]. The structure of the enzymes is similar in water and pure organic solvents because of the high rigidity of the non-polar organic solvents and their inert nature [5–7]. The surface charge distribution and polar residues in the loops are crucial for maintaining the stability of the enzymes in polar organic solvents [8,9]. Organic solvent-tolerant (OST) enzymes have overcome these inactivation challenges and attracted considerable attention as biocatalysts in the presence of organic solvents, including the synthesis of flavors and fragrances, regio- and stereo-selectivity of racemic mixtures, production of biofuels and biodegradable polymers, and recycling/degradation of polymer compounds [10–13]. OST enzymes can also perform synthetic reactions by reversing the thermodynamic equilibrium in organic solvents [11].

OST enzymes have recently been discovered in psychrophiles [14–21]. Cold-adapted OST enzymes are promising biocatalysts for industrial applications at colder temperatures because of the low Gibbs free energy of activation ($\Delta G^{\ddagger}$), resulting from their inherently flexible structures and the stability in organic solvents [22]. Nevertheless, their flexible

structure makes the enzymes susceptible to denaturation at elevated temperatures and high organic solvent concentrations [23]. The effects of polar organic solvents were evident in cold-adapted OST lipases PML and LipS with weaker thermal stability [24]. Introducing new interactions in PML increased the thermal and organic solvent stabilities of PML [25]. On the other hand, not every new interaction improved the organic solvent stability of PML, even though its thermal stability was increased [25]. Studies on thermophilic enzymes also showed that not all thermophilic enzymes are OST enzymes [26,27]. The link between the thermal and organic solvent stabilities of OST enzymes is an important topic in organic solvent enzymology [27], but it has not been fully elucidated.

In this study, the cold-adapted OST lipase PML (EC 3.1.1.3, PDB code 4GW3), an α/β hydrolase with a wide active site [14], was chosen as a model to investigate the roles of intramolecular salt bridges (combination of ionic bonding and hydrogen bonding) in thermal and organic solvent stabilities. The catalytic triad of PML consists of S79, D232, and H254 residues [14]. PML has a substrate preference for *p*-nitrophenyl laurate (*p*NPL) and is tolerant of DMSO, ethanol, and methanol at concentrations up to 50% [24]. Two arginine residues (R237 and R241) on the helix η1 and an aspartate residue (D248) on the connecting loop form salt bridges, thereby stabilizing the catalytic site (Figure 1a). While R237 and D248 are highly conserved in many lipases, R241 is present in PML and forms an additional salt bridge with D248 (Figure 1b). Another basic amino acid residue, histidine, is conserved in the corresponding position of R241 in other lipases (Figure 1b).
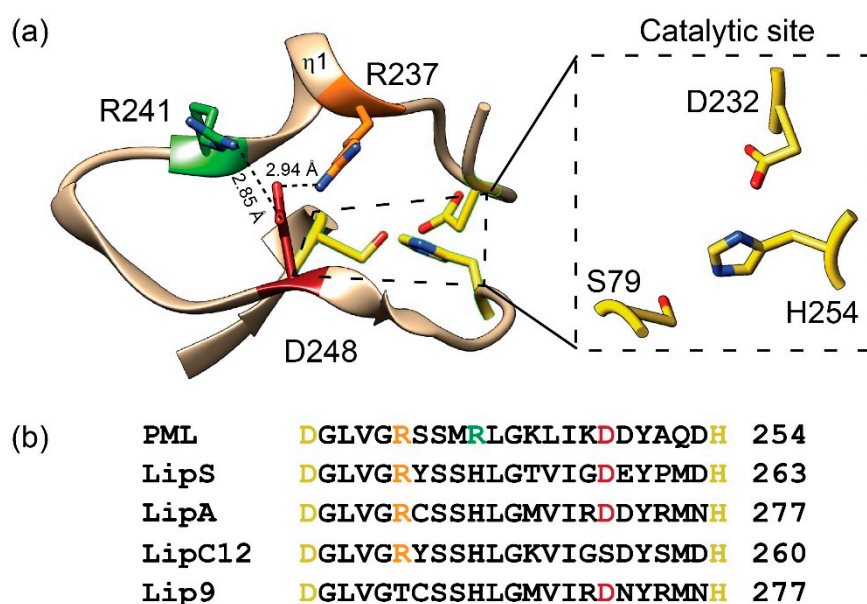

Figure 1. Active-site structure of PML and multiple sequence alignments. (**a**) View of the salt bridges involving R237 and R241 on the helix η1 and D248 on the connecting loop. The catalytic D232 and H254 are located on the connecting loops before and after the helix η1, respectively. (**b**) Multiple sequence alignments of OST lipases. PML [14], LipS [15], LipA [28], LipC12 [29], and Lip9 [30]. Catalytic serine, aspartate, and histidine (yellow), R237 (orange), R241 (green), and D248 (red).

Alanine-scanning mutations were produced in the R237, R241, and D248 residues. A double alanine substitution (R237A/D248) was also generated to confirm the absence of salt bridges. This paper reports that salt bridges holding the active-site catalytic residues of PML in the correct conformation and orientation play a distinct role in maintaining its stability in thermal and organic solvents.

2. Results

2.1. Protein Expression and Purification

The role of the proposed salt bridges in the thermal and organic solvent stabilities of PML was examined by replacing the residues, R237, R241, and D248, with a small aliphatic amino acid, alanine. Hence, four mutants were generated: R237A, R241A, D248A, and R237A/D248A. The wild-type (WT) and mutant PML enzymes were expressed in *E. coli* BL21 (DE3) as soluble proteins. The recombinant PML enzymes were purified to homogeneity by nickel-chelate affinity chromatography followed by Q-Sepharose anion-exchange chromatography (Table 1).

Table 1. Purification summary of the WT and mutant PML enzymes.

		Total Protein (mg)	Total Activity (units)	Specific Activity (units/mg)	Yield (%)	Purity (%)
WT	Cell lysate	121	8935	74	100	25
	HisTrap	14	3457	247	39	83
	Q-Sepharose	11	3269	297	37	100
R237A	Cell lysate	73	8673	119	100	21
	HisTrap	9	4569	508	53	90
	Q-Sepharose	6	3389	565	39	100
R241A	Cell lysate	52	2336	45	100	26
	HisTrap	7	976	139	42	80
	Q-Sepharose	5	874	175	37	100
D248A	Cell lysate	71	3965	56	100	19
	HisTrap	11	2387	217	60	73
	Q-Sepharose	7	2086	298	53	100
R237A/ D248A	Cell lysate	93	10715	115	100	14
	HisTrap	7	4571	653	43	77
	Q-Sepharose	5	4239	848	40	100

Protein concentration was determined by Bradford assay using bovine serum albumin as a standard protein. Enzyme activity was measured as described in the Materials and Methods section.

The recombinant WT and mutant PML enzymes, with an approximately 33 kDa molecular weight, appeared as a single band on an SDS-polyacrylamide gel (Figure 2). The WT and mutant PML enzymes showed the same substrate preference for *p*NPL.
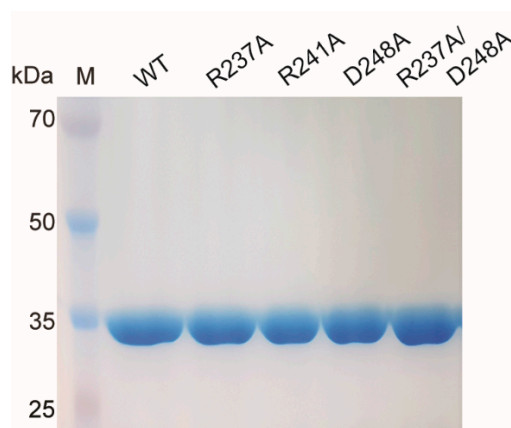

Figure 2. SDS-polyacrylamide gel after purification of WT and mutant PML enzymes using Q-Sepharose anion-exchange chromatography. M—marker.

2.2. Effects of Temperature and Organic Solvent on the Enzymatic Activity

WT PML showed the optimal activity at 35 °C (Figure 3a). The optimal temperature of the R237A and R237A/D248A mutants was 35 °C, whereas the R241A and D248A mutants had a 10 °C lower optimal temperature of 25 °C.
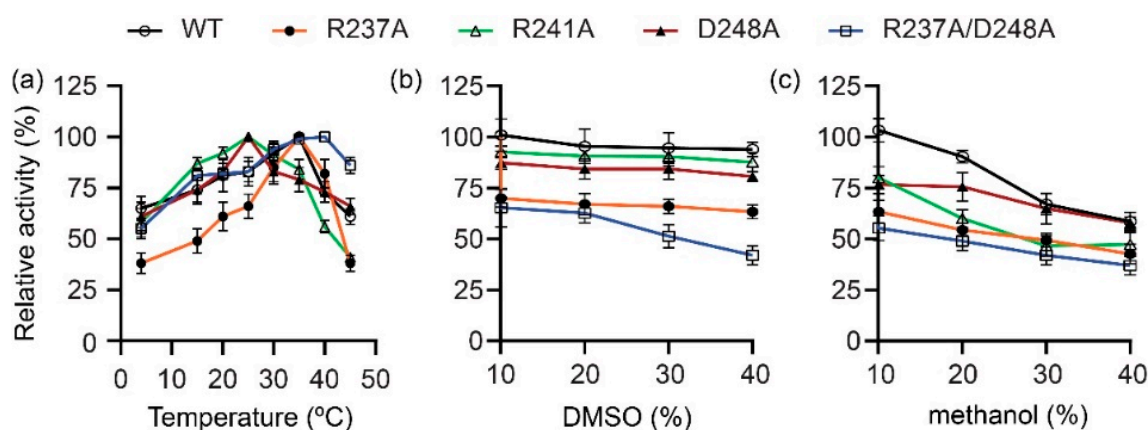
Figure 3. Effects of temperature and organic solvent on the enzymatic activity of WT and mutant PML enzymes. (**a**) Optimum temperature. (**b**) PML activity in 10–40% DMSO. (**c**) PML activity in 10–40% methanol. Data presented correspond to the mean ± SD of three experiments.

The effects of organic solvents on the PML activity were evaluated in 10–40% DMSO and methanol, respectively, at the optimum temperature for 2 min. The enzymatic activity in 10–40% DMSO was in the order of WT ≈ R241A > D248A > R237A > R237A/D248A (Figure 3b). On the other hand, PML mutants showed lower activity in 10–40% methanol than at the same concentrations of DMSO (Figure 3c). Interestingly, the activity of the mutant R241A decreased with increasing methanol concentration (Figure 3c). The double mutant overall showed the lowest enzymatic activity among the mutants in the presence of organic solvents.

2.3. Changes in Conformational Flexibility

As cold-adapted enzymes exhibit an inherently flexible structure, the mutation-induced flexibility changes occurring in PML were assessed using the acrylamide-induced quenching of protein fluorescence in an aqueous buffer (excitation at 280 nm). PML has 1 tryptophan and 15 tyrosine residues. Alanine substitution led to a more flexible structure in all mutants than the WT (Figure 4).
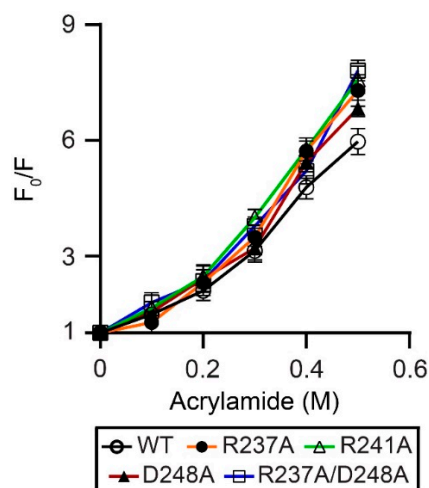
Figure 4. Acrylamide-induced quenching of PML enzyme fluorescence. F_0—the fluorescence intensity in the absence of acrylamide; F—fluorescence intensity in the presence of acrylamide. Data presented correspond to the mean of three experiments.

2.4. Thermal Stability

The thermal stability of the WT and mutant PML enzymes was evaluated under their optimal operating conditions after incubation of the enzymes in an aqueous buffer

at 15–35 °C for 2 h at 30 min intervals (Figure 5). WT maintained 83% activity over the temperature range for 2 h. Although D248A showed similar activity to WT, the activity of other PML mutants decreased with increasing temperature from 15 °C to 35 °C (Figure 5). The thermal stability was in the order of WT ≈ D248A > R237A > R241A > R237A/D248A. As expected, the double mutant R237A/D248A showed the lowest thermal stability among the mutants, exhibiting 65% and 50% activity after incubation at 25 °C and 35 °C for 2 h, respectively. Interestingly, the mutant R241A exhibited reduced thermal stability compared to R237A. These results suggest that the salt bridge involving R241 is more important to the thermal stability of PML than the interactions involving the conserved R237 residue in many lipases.
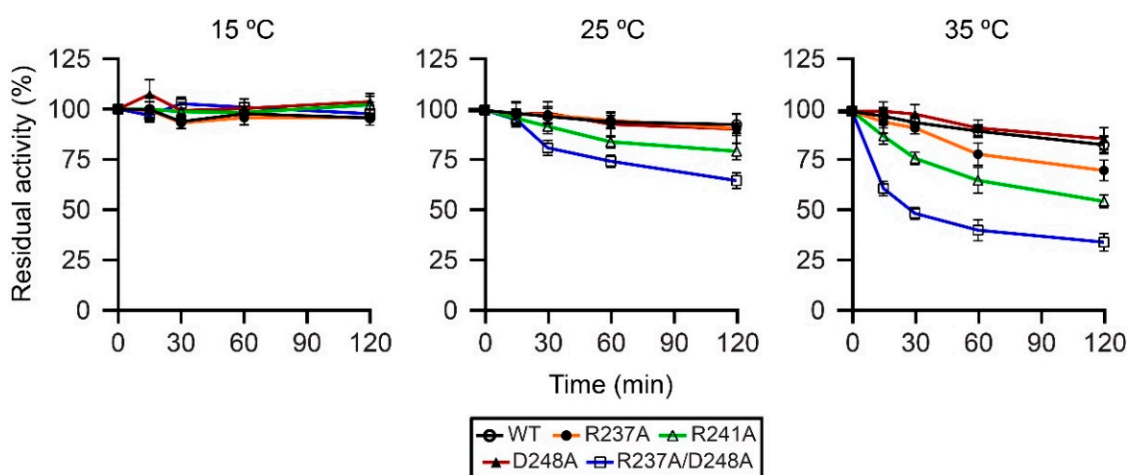

Figure 5. Thermal stability of WT and mutant PML enzymes. Data presented correspond to the mean ± SD of three experiments.

2.5. Organic Solvent Stability

The effects of alanine substitution on the organic solvent stability of WT and mutant PML enzymes were evaluated in 10–40% of DMSO or methanol at 25 °C for up to 3 h (Figure 6). WT maintained its activity quite well in 10–40% DMSO or methanol for 3 h: approximately 83% activity in 40% DMSO and 80% activity in 40% methanol (Figure 6).

On the other hand, the PML mutants showed reduced activity in the presence of DMSO or methanol. The activity of the PML mutants over time decreased with increasing organic solvent concentration (10–40%) (Figure 6). Among the PML mutants, D248A showed the highest activity, while the double mutant R237A/D248A showed the lowest, both in the presence of DMSO or methanol. The results for the PML mutants in 10–30% organic solvents were consistent with the thermal stability profile of the PML mutants (Figure 5). In particular, the double mutant completely lost its activity in 40% DMSO or methanol within 1 h. Although R241A showed slightly lower activity in 10–30% organic solvent than R237A, R237A showed lower activity in 40% organic solvent than R241A. Hence, PML mutants with broken salt bridges involving R237 and R241 are susceptible to denaturation by organic solvents.

The T_m values of the WT and mutant PML enzymes in 10–40% DMSO or methanol were also compared using SYPRO orange-based thermal shift analysis. The T_m value of WT (64.9 °C) was similar to the T_m values of the PML mutants (62.2–65.0 °C) in an aqueous buffer (Table 2). On the other hand, the T_m values of the PML enzymes decreased with increasing DMSO or methanol concentration (Table 2). The WT and mutant PML enzymes showed lower T_m values in 40% DMSO (39.6 °C for WT and 38.9–41.1 °C for the mutants), and even lower T_m values in 40% methanol (36.2 °C for WT and 34.5–36.1 °C for the mutants).
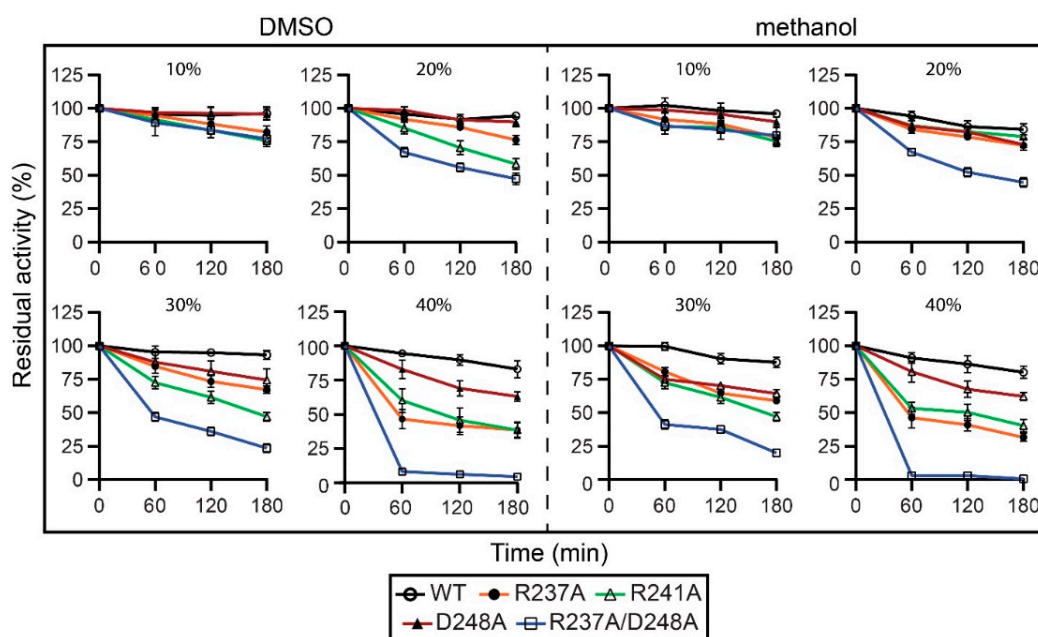
Figure 6. Organic solvent stability of WT and mutant PML enzymes. Stability of PML enzymes in 10–40% DMSO (left panel) and 10–40% methanol (right panel) at 25 °C. Data correspond to the mean ± SD of three experiments.

Table 2. Melting temperature of WT and mutant PML enzymes in 0–40% DMSO and methanol.

	Concentration (%)	T_m (°C)				
		WT	**R237A**	**R241A**	**D248A**	**R237A/D248A**
buffer		64.9 ± 0.3	65.0 ± 0.6	62.2 ± 0.2	62.8 ± 0.1	63.4 ± 0.2
DMSO	10	61.6 ± 0.8	62.1 ± 0.7	63.6 ± 0.3	62.4 ± 0.1	63.1 ± 0.5
	20	56.5 ± 0.6	57.2 ± 0.2	56.1 ± 0.9	57.9 ± 0.4	55.8 ± 0.7
	30	46.5 ± 1.9	46.9 ± 0.4	47.2 ± 0.4	46.3 ± 1.1	45.9 ± 0.9
	40	39.6 ± 1.4	40.3 ± 0.9	38.9 ± 0.7	41.1 ± 0.9	40.8 ± 1.1
methanol	10	60.4 ± 0.9	59.8 ± 0.3	60.7 ± 1.2	59.3 ± 0.5	61.1 ± 0.6
	20	53.4 ± 0.4	54.1 ± 1.3	53.9 ± 0.6	54.5 ± 0.7	54.3 ± 0.9
	30	43.4 ± 1.1	42.7 ± 0.5	43.1 ± 0.8	43.5 ± 1.4	42.8 ± 0.9
	40	36.2 ± 1.7	35.4 ± 2.2	34.5 ± 1.4	36.1 ± 2.3	35.7 ± 1.9

Data presented correspond to the mean ± S.D. of three experiments.

These results are consistent with the activity of PML mutants in 10–40% DMSO and methanol (Figure 3b,c). Interestingly, the loss of salt bridges did not lead to significant changes in the T_m values of the PML mutants compared to those of WT in organic solvents.

2.6. Kinetic and Thermodynamic Properties

Next, the kinetic and thermodynamic properties of WT and mutant PML enzymes were investigated (Table 3). WT showed a K_m value of 370 μM, a k_{cat} value of 59 s^{-1}, and a kinetic efficiency of 0.16 s^{-1}μM^{-1} at 25 °C. Alanine substitution did not significantly affect the kinetic parameters of R237A and R241A, but D248A showed a 2.1-fold lower K_m value while maintaining a similar k_{cat} value to that of WT, which led to a 1.9-fold higher catalytic efficiency. Interestingly, the double mutant, R237A/D248A, showed a 1.9-fold higher K_m value and 4.0-fold higher k_{cat} value, leading to a 2-fold higher catalytic efficiency than WT. This observation is consistent with the increased conformational flexibility of the double mutant and its reduced stability in 10–40% DMSO or methanol and elevated temperatures. Hence, the salt bridges are responsible for maintaining the active-site stability of PML.

**Table 3.** Kinetic and thermodynamic parameters of WT and mutant PML enzymes.

	K_m (μM)	k_{cat} (S^{-1})	k_{cat}/K_m (μM^{-1} S^{-1})	ΔG‡ (kJ mol^{-1})	ΔH‡ (kJ mol^{-1})	TΔS‡ (kJ mol^{-1})
WT	370 ± 12	59 ± 4	0.16 ± 0.02	64.0	17.4	−46.6
R237A	241 ± 7	42 ± 1	0.18 ± 0.01	62.3	17.4	−44.9
R241A	234 ± 15	58 ± 9	0.24 ± 0.03	64.2	17.3	−46.9
D248A	177 + 21	53 ± 8	0.30 ± 0.10	64.3	12.8	−51.5
R237A/ D248A	716 ± 42	234 ± 10	0.32 ± 0.40	56.5	10.6	−45.8

Data presented correspond to the mean ± S.D. of three experiments.

The Gibbs free energy of activation (ΔG‡), enthalpy of activation (ΔH‡), and entropy (TΔS‡) of WT were determined to be 64 kJ mol^{-1}, 17.4 kJ mol^{-1}, and −46.6 kJ mol^{-1}, respectively. Single alanine substitution did not affect the thermodynamic properties of R237A and R241A. D248A showed a larger TΔS‡ value (–51.5 kJ/mol), indicating a substantial change in its active-site structure, but the mutation did not lead to increased catalytic activity. On the other hand, the double mutant, R237A/D247A, showed a lower ΔG‡ value (64.3 kJ mol^{-1}) compared to WT and other mutants, which is consistent with its higher catalytic rate, but did not show a flexible active-site structure from its TΔS‡ value (−45.8 kJ mol^{-1}).

2.7. Circular Dichroism (CD) Spectra Analysis

The CD spectra were measured to evaluate the mutation-induced secondary structure changes in the WT and mutant PML enzymes (Figure 7).
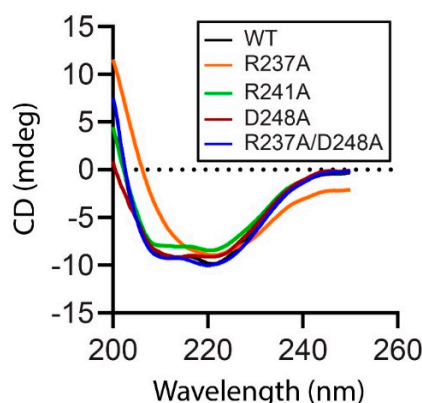
Figure 7. CD spectra of WT and mutant PML enzymes.

WT consisted mainly of α-helices (46.3%) with a minor portion of β-strands (5.7%). The PML mutants (R241A, D248A, and R237A/D248A) had α-helix and β-strand contents similar to WT PML. On the other hand, R237A showed a different CD spectrum than WT and the other PML mutants, with a 1.28-fold higher α-helix content (59.4%) but a slightly lower β-strand content (4.5%).

3. Discussion

Considerable efforts have been made to increase the stability of native enzymes in organic solvents for industrial applications [10,31]. Since the identification of the first OST lipase Lip9 from *Pseudomonas aeruginosa* LST-03 [30], OST enzymes have been reported in psychrophiles. Cold-adapted enzymes generally exhibit reduced intramolecular interactions and show intrinsically flexible structures [32,33]. In particular, cold-adapted enzymes exhibit a higher lysine/arginine ratio, lower proline content, glycine clustering at catalytic site, and increased loop length [34]. Arginine participates in the formation of more hydrogen bonds and ionic interactions than lysine, whereas proline reduces the structural flexibility. The reduced surface hydrophobicity of cold-adapted enzymes provides

tight binding of surface charged and polar residues to available water molecules, thereby increasing its OST property [35]. Directed evolution has been more successful in attaining a thermal and increasing organic solvent stability than rational design because the hot spots of mutation are not easily identified [31,36]. Introducing charged residues on the protein surface via directed evolution further increased the stability of the OST enzymes in polar organic solvents [31,37].

Despite the active site being more flexible than the overall protein structure in cold-adapted enzymes [38], the active site should maintain the correct conformation and orientation of the catalytic residues [39]. The residues surrounding the catalytic site help provide the correct spatial relationship. The salt bridge that stabilizes the α-helix with catalytic aspartate and the β-strand with catalytic histidine (the interaction between R237 and D248 in PML) is highly conserved in many esterases, including hyperthermophilic esterase EstE1 (optimal temperature 70 °C) and mesophilic esterase rPPE (optimal temperature 50 °C) [40]. The disruption of the salt bridge in the structurally rigid EstE1 increased the conformational flexibility of the protein significantly but had a lesser effect on the thermal stability [40]. In contrast, the disruption of the salt bridge in the relatively flexible rPPE had a lesser effect on the conformational flexibility but resulted in reduced thermal stability [40]. These results are consistent with those on rPPE in that the alanine-substituted PML mutants showed a larger change in thermal stability than conformational flexibility in an aqueous buffer because the structure of PML is intrinsically flexible. Alanine substitution also affected the conformation and stability of the PML mutants. Specifically, R237A showed a 1.28-fold increase in α-helical content by mutations despite no change in the T_m value compared to WT. On the other hand, the other PML mutants showed 1.6–2.8 °C lower T_m values despite the similar α-helical content to WT.

Several studies showed that intramolecular interactions for both the thermal and organic solvent stabilities of enzymes differ [25,27,41]. On the other hand, the specific interactions in the enzyme active site responsible for the stability in an organic solvent have not been elucidated. These results show that the salt bridges involving R237, R241, and D248 play a more important role in the active-site stability of PML in organic solvents than at elevated temperatures. The interactions of the organic solvents with enzymes are weak and non-specific as the effect of organic solvents is only noticeable at high concentrations, and the organic solvent itself does not bind to a specific site on the enzyme [42]. Polar organic solvents exhibit detrimental effects on the stability of proteins, while enzymes are more tolerant of non-polar organic solvents. DMSO is a polar aprotic solvent, and DMSO above a certain concentration shows significant perturbations of protein secondary structure by interfering with the intramolecular backbone C = O···H–N bonds [43]. On the other hand, DMSO can also increase the enzyme activity by reducing aggregation [44]. By contrast, as a polar protic solvent, methanol can interact with the protein via the hydrophobic interactions and hydrogen bonding, thus destabilizing enzyme structure [45,46]. The similar but distinct properties of DMSO and methanol exert different stability profiles of PML mutants in organic solvents. DMSO and methanol lowered the T_m values of the PML WT and mutants, as expected, in the order of aqueous buffer > DMSO > methanol. Considering that the active site is the least stable structural element in cold-adapted enzymes [38], these results suggest that direct interactions of DMSO and methanol with the residues near the active site can have a more detrimental effect on the structure of PML compared to the global effect of heat on the protein structure.

The structure of PML shows that R237 and R241 form ionic interactions with D248, and also hydrogen bonds with Q230 and G182, respectively (Figure 8). Although another aspartate residue D249 is located next to D248, the structure of PML suggests that the side chain of D249 is more likely to form a salt bridge with the side chain of K247 (2.7 Å) rather than with the side chain of R237 (5.4 Å) (Figure 8). Among the mutants, D248A showed similar thermal stability to the WT but reduced solvent stability in DMSO and methanol (Figures 5 and 6). These hydrogen bond formations between R237 and Q230 and between R241 and G182 support the similar thermal stability of D248A to the WT.
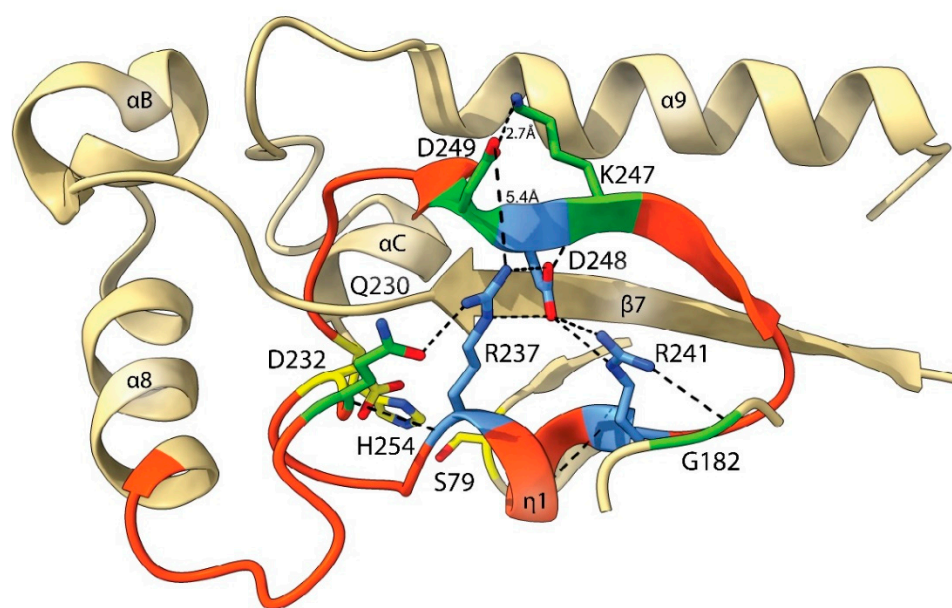
Figure 8. Enlarged view of the active-site region of PML. In addition to the ion pair formation with D248, R237 and R241 also form hydrogen bonds with Q230 and G182, respectively. S79, D232, and H254 are the catalytic residues.

In conclusion, the conformational changes within the cold-adapted OST lipase PML, involving salt bridges near the active site, have distinct effects on the thermal and organic solvent stabilities of PML, with a larger effect on the organic solvent stability than the thermal stability. The differences between the thermal and organic solvent stabilities of OST enzymes may be distinguished further using intrinsically flexible cold-adapted OST enzymes and molecular dynamics simulations.

4. Materials and Methods

4.1. Materials

The *pml* gene with a C-terminal six histidine-tag was synthesized at GenScript (Piscataway, NJ, USA). *Pfu* polymerase and restriction enzymes were purchased from Enzynomics (Daejeon, South Korea), HisTrap, Desalting, and Q-Sepharose columns were acquired from GE Healthcare (Piscataway, NJ, USA). The pET28a(+) expression vector was obtained from Novagen (Madison, WI, USA). *p*-Nitrophenyl laurate (*p*NPL) was purchased from Sigma (St. Louis, MO, USA). All other reagents were from Sigma unless noted otherwise.

4.2. Structural Modelling

The structural models of the PML mutants were constructed using the Swiss Model (https://swissmodel.expasy.org, accessed on 1 June 2022) based on the crystal structure of PML (PDB code 4GW3) [14]. The molecular graphics program UCSF Chimera was used to display the structure of WT and mutant PML enzymes [47].

4.3. Site-Directed Mutagenesis

Alanine substitution of the PML mutants was generated by *Pfu* polymerase-based site-directed mutagenesis using the following primers.

R237A   5′-CTTAGTTGGTG**GCC**TCGAGTATG-3′ and
5′-CATACTCGA**GGC**ACCAACTAAG-3′
R241A   5′-GCTCGAGTATG**GCA**TTAGGTAAATTG-3′ and
5′-CAATTTACCTAA**TGC**CATACTCGAGC-3′
D248A   5′-GATAAAG**GCT**GATTATGCGC-3′ and 5′-GCGCATAATC**AGC**CTTTATC-3′

For the generation of the double mutant R237A/D248A, the primers for D248A were used for a polymerase chain reaction using the nucleotide sequence of R237A as a tem-

plate. Mutated codons are underlined. The presence of mutation was confirmed by DNA sequencing after PCR and subcloning.

4.4. Protein Expression and Purification

After subcloning genes into the pET28a(+) vector, recombinant WT and mutant PML enzymes were expressed in *Escherichia coli* BL21 (DE3). A single colony of *E. coli* BL21 (DE3) grown on an LB/kanamycin plate was picked to grow overnight to form the starting culture. After the addition of 1% of the starting culture to 100 mL of freshly prepared LB broth, cells were propagated at 37 °C until they reached the mid-log phase (OD$_{600}$ = 0.6–0.8). The growth temperature was then lowered to 18 °C and 1 mM isopropyl β-D-1-thiogalactopyranoside (IPTG) was added. Cells growth was continued for an additional 16 h after the IPTG induction.

After harvesting the cells at 13,000× *g* for 10 min, cells were ruptured by sonication in buffer A (20 mM Tris HCl, pH 7.5, 100 mM NaCl, and 5% glycerol) and the centrifugation-recovered lysate supernatant. Imidazole concentration was adjusted to 5 mM for nickel-chelate affinity chromatography. The WT and mutant PML enzymes were purified using a 1 mL HisTrap column with a step gradient (100 mM and 500 mM imidazole) in buffer A on an AKTA Explorer system (GE Healthcare, Piscataway, NJ, USA). Next, the proteins were further purified using a 1 mL Q-Sepharose column with a linear gradient of 25 to 1000 mM KCl in buffer B (25 mM Tris HCl, pH 7.5, 25 mM KCl, and 5% glycerol). All purification steps were conducted at 4 °C. Purified enzymes were stored at −80 °C by flash freezing them in liquid nitrogen.

4.5. Enzyme Assay and Thermal Stability

Enzyme activity of WT and mutant PML enzymes was determined in reaction buffer (100 mM Tris HCl, pH 8.0, 100 mM NaCl, and 5% glycerol) with *p*NPL using a Shimadzu UV-1800 spectrophotometer (Kyoto, Japan) at 405 nm with a final subtraction of the background hydrolysis of *p*NP esters. The optimal temperature of the enzyme was measured at 4–45 °C for 2 min. The thermal stability of the enzymes was determined by measuring the residual activity at the optimum temperature upon incubation of the enzymes at various temperatures (15–35 °C) for the indicated times (every 15 min interval for up to 2 h).

4.6. Activity and Stability in Organic Solvents

Activities of PML enzymes were determined in the reaction buffer containing 10–40% DMSO or methanol at the optimum temperature for 2 min. The organic solvent stability of the PML enzymes was determined by measuring the residual activity at the optimum temperature upon incubation of the enzymes in the reaction buffer with 10–40% DMSO or methanol at 25 °C for the indicated times (every 60 min interval for up to 3 h). The organic solvent concentration in the reaction buffer was maintained at 2% while measuring the residual activity. Enzymatic activity without organic solvent presence was used as a control.

4.7. Enzyme Kinetics and Thermodynamics Analysis

Kinetics of WT and mutant PML enzymes were determined at the optimum temperature of the WT enzyme (35 °C). The Michaelis constant (K_m) and the catalytic rate constant (k_{cat}) were measured from Lineweaver-Burk plots. The Arrhenius plot was constructed using k_{cat} values measured at different temperatures (4 °C, 15 °C, 25 °C, 30 °C, and 35 °C). The activation energy (E_a) of *p*NPL was calculated from the Arrhenius plot. Thermodynamic parameters, including Gibbs free energy of activation ($\Delta G^{\ddagger}$), enthalpy ($\Delta H^{\ddagger}$), and entropy ($T\Delta S^{\ddagger}$), were determined using the following equations.

$$\Delta G^{\ddagger} = RT \times \left[\ln\left(\frac{k_B T}{h} \right) - \ln k \right]$$

$$\Delta H^{\ddagger} = E_a - RT$$

$$\Delta S^{\ddagger} = \left(\Delta H^{\ddagger} - \Delta G^{\ddagger} \right) / T$$

where k_B is the Boltzmann constant (1.3805×10^{-23} J K^{-1}), h is the Planck constant (6.6256×10^{-34} J s), k is the catalytic rate constant, and R is the universal gas constant (8.314 J mol^{-1} K^{-1}).

4.8. Protein Thermal Shift Analysis

The SYPRO orange dye-based thermal shift assay was conducted on an Applied Biosystems StepOnePlus real-time PCR system (Waltham, MA, USA). Sample mixture with or without DMSO or methanol contained approximately 20 µM of protein in the incubation buffer (100 mM Tris·HCl, pH 7.5, and 100 mM NaCl) with a $1\times$ final concentration of SYPRO orange dye. Melting temperature (T_m) of the enzyme was recorded from within the temperature range of 25–95 °C with a 1 °C increase per minute. Data were analyzed using protein thermal shift software from Thermo Fisher (Waltham, MA, USA).

4.9. Quenching of Protein Fluorescence

Acrylamide-induced fluorescence quenching was measured using a Scinco FS-2 fluorescence spectrometer (Seoul, Korea) at 25 °C. Initially, 10 µmol of protein was added to buffer containing 0–40% DMSO or methanol. The fluorescence of the protein from tryptophan and tyrosine residues was measured at 280 nm upon addition of increasing concentrations of acrylamide (0–0.5 M). Quenching data are presented as a proportion of the intrinsic fluorescence intensity (F_0) to the fluorescence intensity in the presence of 0–0.5 M acrylamide (F).

4.10. CD Spectroscopy

The secondary structure of the WT and mutant PML enzymes was determined using a JASCO J-1500 spectropolarimeter (Tokyo, Japan), which was available at the Korea Basic Science Institute (Ochang, Korea). Protein samples (0.5 mg/mL) in buffer B were incubated at 25 °C for 1 h before measuring CD spectra. The data were analyzed using K2D3, a web server that analyzes protein secondary structure [48].

References

1. Klibanov, A.M. Improving enzymes by using them in organic solvents. *Nature* **2001**, *409*, 241–246. [CrossRef] [PubMed]
2. Klibanov, A.M. Why are enzymes less active in organic solvents than in water? *Trends Biotechnol.* **1997**, *15*, 97–101. [CrossRef]
3. Gorman, L.A.; Dordick, J.S. Organic solvents strip water off enzymes. *Biotechnol. Bioeng.* **1992**, *39*, 392–397. [CrossRef] [PubMed]
4. Stepankova, V.; Damborsky, J.; Chaloupkova, R. Organic co-solvents affect activity, stability and enantioselectivity of haloalkane dehalogenases. *Biotechnol. J.* **2013**, *8*, 719–729. [CrossRef]
5. Kamal, M.Z.; Yedavalli, P.; Deshmukh, M.V.; Rao, N.M. Lipase in aqueous-polar organic solvents: Activity, structure, and stability. *Protein Sci.* **2013**, *22*, 904–915. [CrossRef]
6. Fitzpatrick, P.A.; Ringe, D.; Klibanov, A.M. X-ray crystal structure of cross-linked subtilisin Carlsberg in water vs. acetonitrile. *Biochem. Biophys. Res. Commun.* **1994**, *198*, 675–681. [CrossRef]
7. Allen, K.N.; Bellamacina, C.R.; Ding, X.; Jeffery, C.J.; Mattos, C.; Petsko, G.A.; Ringe, D. An experimental approach to mapping the binding surfaces of crystalline proteins. *J. Phys. Chem.* **1996**, *100*, 2605–2611. [CrossRef]

8.   Chakravorty, D.; Parameswaran, S.; Dubey, V.K.; Patra, S. Unraveling the rationale behind organic solvent stability of lipases. *Appl. Biochem. Biotechnol.* **2012**, *167*, 439–461. [CrossRef]

9.   Yedavalli, P.; Rao, N.M. Engineering the loops in a lipase for stability in DMSO. *Protein Eng. Des. Sel.* **2013**, *26*, 317–324. [CrossRef]

10. Stepankova, V.; Bidmanova, S.; Koudelakova, T.; Prokop, Z.; Chaloupkova, R.; Damborsky, J. Strategies for stabilization of enzymes in organic solvents. *ACS Catal.* **2013**, *3*, 2823–2836. [CrossRef]

11. Kumar, A.; Dhar, K.; Kanwar, S.S.; Arora, P.K. Lipase catalysis in organic solvents: Advantages and applications. *Biol. Proced. Online* **2016**, *18*, 2. [CrossRef] [PubMed]

12. Priyanka, P.; Tan, Y.; Kinsella, G.K.; Henehan, G.T.; Ryan, B.J. Solvent stable microbial lipases: Current understanding and biotechnological applications. *Biotechnol. Lett.* **2019**, *41*, 203–220. [CrossRef] [PubMed]

13. Doukyu, N.; Ogino, H. Organic solvent-tolerant enzymes. *Biochem. Eng. J.* **2010**, *48*, 270–282. [CrossRef]

14. Korman, T.P.; Bowie, J.U. Crystal structure of Proteus mirabilis lipase, a novel lipase from the Proteus/psychrophilic subfamily of lipase family I.1. *PLoS ONE* **2012**, *7*, e52890. [CrossRef]

15. Kim, J.; Jang, S.H.; Lee, C. An organic solvent-tolerant alkaline lipase from cold-adapted Pseudomonas mandelii: Cloning, expression, and characterization. *Biosci. Biotechnol. Biochem.* **2013**, *77*, 320–323. [CrossRef] [PubMed]

16. Dachuri, V.K.; Lee, C.; Jang, S.H. Organic solvent-tolerant esterase from Sphingomonas glacialis based on amino acid composition analysis: Cloning and characterization of EstSP2. *J. Microbiol. Biotechnol.* **2018**, *28*, 1502–1510. [CrossRef] [PubMed]

17. Hong, D.K.; Jang, S.-H.; Lee, C. Gene cloning and characterization of a psychrophilic phthalate esterase with organic solvent tolerance from an Arctic bacterium Sphingomonas glacialis PAMC 26605. *J. Mol. Catal. B Enzym.* **2016**, *133*, S337–S345. [CrossRef]

18. Guo, H.; Zhang, Y.; Shao, Y.; Chen, W.; Chen, F.; Li, M. Cloning, expression and characterization of a novel cold-active and organic solvent-tolerant esterase from Monascus ruber M7. *Extremophiles* **2016**, *20*, 451–459. [CrossRef]

19. Ganasen, M.; Yaacob, N.; Rahman, R.N.; Leow, A.T.; Basri, M.; Salleh, A.B.; Ali, M.S. Cold-adapted organic solvent tolerant alkalophilic family I.3 lipase from an Antarctic Pseudomonas. *Int. J. Biol. Macromol.* **2016**, *92*, 1266–1276. [CrossRef]

20. Yamashiro, Y.; Sakatoku, A.; Tanaka, D.; Nakamura, S. A cold-adapted and organic solvent-tolerant lipase from a psychrotrophic bacterium Pseudomonas sp. strain YY31: Identification, cloning, and characterization. *Appl. Biochem. Biotechnol.* **2013**, *171*, 989–1000. [CrossRef]

21. Ji, Q.; Xiao, S.; He, B.; Liu, X. Purification and characterization of an organic solvent-tolerant lipase from Pseudomonas aeruginosa LX1 and its application for biodiesel production. *J. Mol. Catal. B Enzym.* **2010**, *66*, 264–269. [CrossRef]

22. Santiago, M.; Ramirez-Sarmiento, C.A.; Zamora, R.A.; Parra, L.P. Discovery, molecular mechanisms, and industrial applications of cold-active enzymes. *Front. Microbiol.* **2016**, *7*, 1408. [CrossRef] [PubMed]

23. Lee, C.; Jang, S.-H.; Chung, H.-S. Improving the stability of cold-adapted enzymes by immobilization. *Catalysts* **2017**, *7*, 112. [CrossRef]

24. Dachuri, V.; Boyineni, J.; Choi, S.; Chung, H.-S.; Jang, S.-H.; Lee, C. Organic solvent-tolerant, cold-adapted lipases PML and LipS exhibit increased conformational flexibility in polar organic solvents. *J. Mol. Catal. B Enzym.* **2016**, *131*, 73–78. [CrossRef]

25. Korman, T.P.; Sahachartsiri, B.; Charbonneau, D.M.; Huang, G.L.; Beauregard, M.; Bowie, J.U. Dieselzymes: Development of a stable and methanol tolerant lipase for biodiesel production by directed evolution. *Biotechnol. Biofuels* **2013**, *6*, 70. [CrossRef] [PubMed]

26. Karshikoff, A.; Nilsson, L.; Ladenstein, R. Rigidity versus flexibility: The dilemma of understanding protein thermal stability. *FEBS J.* **2015**, *282*, 3899–3917. [CrossRef]

27. Shehata, M.; Timucin, E.; Venturini, A.; Sezerman, O.U. Understanding thermal and organic solvent stability of thermoalkalophilic lipases: Insights from computational predictions and experiments. *J. Mol. Model.* **2020**, *26*, 122. [CrossRef]

28. Zha, D.; Xu, L.; Zhang, H.; Yan, Y. Molecular identification of lipase LipA from Pseudomonas protegens Pf-5 and characterization of two whole-cell biocatalysts Pf-5 and Top10lipA. *J. Microbiol. Biotechnol.* **2014**, *24*, 619–628. [CrossRef]

29. Glogauer, A.; Martini, V.P.; Faoro, H.; Couto, G.H.; Müller-Santos, M.; Monteiro, R.A.; Mitchell, D.A.; de Souza, E.M.; Pedrosa, F.O.; Krieger, N. Identification and characterization of a new true lipase isolated through metagenomic approach. *Microb Cell Fact* **2011**, *10*, 54. [CrossRef]

30. Ogino, H.; Miyamoto, K.; Ishikawa, H. Organic-solvent-tolerant bacterium which secretes organic-solvent-stable lipolytic enzyme. *Appl. Environ. Microbiol.* **1994**, *60*, 3884–3886. [CrossRef]

31. Cui, H.; Stadtmüller, T.H.J.; Jiang, Q.; Jaeger, K.-E.; Schwaneberg, U.; Davari, M.D. How to engineer organic solvent resistant enzymes: Insights from combined molecular dynamics and directed evolution study. *ChemCatChem* **2020**, *12*, 4073–4083. [CrossRef]

32. Parvizpour, S.; Hussin, N.; Shamsir, M.S.; Razmara, J. Psychrophilic enzymes: Structural adaptation, pharmaceutical and industrial applications. *Appl. Microbiol. Biotechnol.* **2021**, *105*, 899–907. [CrossRef] [PubMed]

33. Mhetras, N.; Mapare, V.; Gokhale, D. Cold active lipases: Biocatalytic tools for greener technology. *Appl. Biochem. Biotechnol.* **2021**, *193*, 2245–2266. [CrossRef]

34. De Maayer, P.; Anderson, D.; Cary, C.; Cowan, D.A. Some like it cold: Understanding the survival strategies of psychrophiles. *EMBO Rep.* **2014**, *15*, 508–517. [CrossRef]

35. Karan, R.; Capes, M.D.; Dassarma, S. Function and biotechnology of extremophilic enzymes in low water activity. *Aquat. Biosyst.* **2012**, *8*, 4. [CrossRef] [PubMed]

36. Markel, U.; Zhu, L.; Frauenkron-Machedjou, V.J.; Zhao, J.; Bocola, M.; Davari, M.D.; Jaeger, K.-E.; Schwaneberg, U. Are directed evolution approaches efficient in exploring nature's potential to stabilize a lipase in organic cosolvents? *Catalysts* **2017**, *7*, 142. [CrossRef]

37. Kawata, T.; Ogino, H. Enhancement of the organic solvent-stability of the LST-03 lipase by directed evolution. *Biotechnol Prog.* **2009**, *25*, 1605–1611. [CrossRef] [PubMed]

38. Siddiqui, K.S.; Feller, G.; D'Amico, S.; Gerday, C.; Giaquinto, L.; Cavicchioli, R. The active site is the least stable structure in the unfolding pathway of a multidomain cold-adapted alpha-amylase. *J. Bacteriol.* **2005**, *187*, 6197–6205. [CrossRef]

39. Truongvan, N.; Jang, S.H.; Lee, C. Flexibility and stability trade-off in active site of cold-adapted Pseudomonas mandelii esterase EstK. *Biochemistry* **2016**, *55*, 3542–3549. [CrossRef]

40. Dachuri, V.; Truongvan, N.; DangThu, Q.; Jang, S.H.; Lee, C. Distinct roles of an ionic interaction holding an alpha-helix with catalytic Asp and a beta-strand with catalytic His in a hyperthermophilic esterase EstE1 and a mesophilic esterase rPPE. *Extremophiles* **2019**, *23*, 649–657. [CrossRef]

41. Zaks, A.; Klibanov, A.M. Enzymatic catalysis in organic media at 100 degrees C. *Science* **1984**, *224*, 1249–1251. [CrossRef] [PubMed]

42. Canchi, D.R.; Garcia, A.E. Cosolvent effects on protein stability. *Annu. Rev. Phys. Chem.* **2013**, *64*, 273–293. [CrossRef] [PubMed]

43. Jackson, M.; Mantsch, H.H. Beware of proteins in DMSO. *Biochim. Biophys. Acta* **1991**, *1078*, 231–235. [CrossRef]

44. Ferreira, J.C.; Fadl, S.; Ilter, M.; Pekel, H.; Rezgui, R.; Sensoy, O.; Rabeh, W.M. Dimethyl sulfoxide reduces the stability but enhances catalytic activity of the main SARS-CoV-2 protease 3CLpro. *FASEB J.* **2021**, *35*, e21774. [CrossRef] [PubMed]

45. Hwang, S.; Shao, Q.; Williams, H.; Hilty, C.; Gao, Y.Q. Methanol strengthens hydrogen bonds and weakens hydrophobic interactions in proteins—A combined molecular dynamics and NMR study. *J. Phys. Chem. B* **2011**, *115*, 6653–6660. [CrossRef] [PubMed]

46. Pazhang, M.; Mardi, N.; Mehrnejad, F.; Chaparzadeh, N. The combinatorial effects of osmolytes and alcohols on the stability of pyrazinamidase: Methanol affects the enzyme stability through hydrophobic interactions and hydrogen bonds. *Int. J. Biol. Macromol.* **2018**, *108*, 1339–1347. [CrossRef]

47. Pettersen, E.F.; Goddard, T.D.; Huang, C.C.; Couch, G.S.; Greenblatt, D.M.; Meng, E.C.; Ferrin, T.E. UCSF Chimera—A visualization system for exploratory research and analysis. *J. Comput. Chem.* **2004**, *25*, 1605–1612. [CrossRef]

48. Louis-Jeune, C.; Andrade-Navarro, M.A.; Perez-Iratxeta, C. Prediction of protein secondary structure from circular dichroism using theoretically derived spectra. *Proteins* **2012**, *80*, 374–381. [CrossRef]